

# Electronic correlations and Hund's coupling effects in SrMoO<sub>3</sub> revealed by photoemission spectroscopy

H. Wadati,<sup>1,\*</sup> K. Yoshimatsu,<sup>2</sup> H. Kumigashira,<sup>2</sup> M. Oshima,<sup>2</sup> T. Sugiyama,<sup>3</sup> E. Ikenaga,<sup>3</sup> A. Fujimori,<sup>4</sup> J. Mravlje,<sup>5,6,7</sup> A. Georges,<sup>6,7,8</sup> A. Radetinac,<sup>9</sup> K. S. Takahashi,<sup>10</sup> M. Kawasaki,<sup>1,10</sup> and Y. Tokura<sup>1,10</sup>

<sup>1</sup>*Department of Applied Physics and Quantum-Phase Electronics Center (QPEC), University of Tokyo, Hongo, Tokyo 113-8656, Japan*

<sup>2</sup>*Department of Applied Chemistry, University of Tokyo, Bunkyo-ku, Tokyo 113-8656, Japan*

<sup>3</sup>*Japan Synchrotron Radiation Research Institute, SPring-8, Hyogo 679-5198, Japan*

<sup>4</sup>*Department of Physics, University of Tokyo, Bunkyo-ku, Tokyo 113-0033, Japan*

<sup>5</sup>*Jozef Stefan Institute, Jamova 39, Ljubljana, Slovenia*

<sup>6</sup>*Collège de France, 11 place Marcelin Berthelot, 75005 Paris, France*

<sup>7</sup>*Centre de Physique Théorique, École Polytechnique, CNRS, 91128 Palaiseau, France*

<sup>8</sup>*DPMC, Université de Genève, 24 quai Ernest-Ansermet, 1211 Genève 4, Switzerland*

<sup>9</sup>*Institut für Materialwissenschaft, Technische Universität Darmstadt, Petersenstrabe 23, 64287 Darmstadt, Germany*

<sup>10</sup>*RIKEN Center for Emergent Matter Science (CEMS), Wako 351-0198, Japan*

(Dated: January 27, 2014)

We investigate the electronic structure of a perovskite-type Pauli paramagnet SrMoO<sub>3</sub> ( $t_{2g}^2$ ) thin film using hard x-ray photoemission spectroscopy and compare the results to the realistic calculations that combine the density functional theory within the local-density approximation (LDA) with the dynamical-mean field theory (DMFT). Despite the clear signature of electron correlations in the electronic specific heat, the narrowing of the quasiparticle bands is not observed in the photoemission spectrum. This is explained in terms of the characteristic effect of Hund's rule coupling for partially-filled  $t_{2g}$  bands, which induces strong quasiparticle renormalization already for values of Hubbard interaction which are smaller than the bandwidth. The interpretation is supported by additional model DMFT calculations including Hund's rule coupling, that show renormalization of low-energy quasiparticles without affecting the overall bandwidth. The photoemission spectra show additional spectral weight around  $-2$  eV that is not present in the LDA+DMFT. We interpret this weight as a plasmon satellite, which is supported by measured Mo, Sr and Oxygen core-hole spectra that all show satellites at this energy.

## I. INTRODUCTION

Electron correlation in transition-metal oxides (TMOs) has been the subject of extensive studies in recent decades<sup>1</sup>. Photoemission spectroscopy has made major contributions to a better understanding of electron correlation effects in those materials. Perovskite-type SrVO<sub>3</sub> has been extensively studied as a prototypical correlated system with the  $t_{2g}^1$  configuration and no magnetism<sup>2,3</sup>. The bulk spectrum of the V  $3d$  bands was obtained by using soft x-ray (SX) photoemission spectroscopy and it was found that the width of the coherent part (quasiparticle band)  $W^*$  is reduced to about half of that found in the band-structure calculation  $W_b$ <sup>4</sup>, that is,  $W_b/W^* \sim 2$ . This is consistent with specific heat measurements, which suggest  $m^*/m_b = \gamma/\gamma_b \sim 2$ , where  $\gamma$  is the experimental specific heat coefficient,  $\gamma_b$  is the theoretical specific heat coefficient obtained from the band-structure calculations,  $m^*$  is the effective mass of the quasiparticle, and  $m_b$  is the bare band mass<sup>5</sup>. The photoemission spectra also displayed a clear lower Hubbard band. Such a photoemission signal with well-separated Hubbard bands and a narrow quasiparticle peak has become an icon of correlated electron materials.

Surprisingly, the situation in TMOs with more than one  $d$  electron has been found to be quite different. Among such systems, SrRuO<sub>3</sub> ( $t_{2g}^4$ ) has attracted par-

ticular interest due to the metallicity and ferromagnetism with  $T_C \sim 160$  K<sup>6</sup>. Takizawa *et al.*<sup>7</sup> obtained a bulk Ru  $4d$  spectrum of SrRuO<sub>3</sub> through SX photoemission studies of *in situ* prepared thin films, and found that the bandwidths found in the experimental bulk spectrum agree with those found in the band-structure calculation, that is,  $W_b/W^* \sim 1$ . This result, however, now does not match  $m^*/m_b = \gamma/\gamma_b \sim 4$  found from specific heat measurements<sup>8,9</sup>, which lead Takizawa *et al.* to a conclusion that the genuine coherent part with the renormalized electron mass exists only in the vicinity of the Fermi level ( $E_F$ ). In another  $t_{2g}^4$  system Sr<sub>2</sub>RuO<sub>4</sub>, which is a layered superconductor<sup>10</sup>, the situation is quite similar to SrRuO<sub>3</sub> in the sense that  $W_b/W^* \sim 1$  but  $m^*/m_b = \gamma/\gamma_b \sim 4^{10-12}$ . These facts are summarized in Table I. The absence of pronounced Hubbard bands in the photoemission spectra of ruthenates led some of the researchers in the field to adopt the extreme view that electronic correlations are altogether absent or negligible in SrRuO<sub>3</sub> and CaRuO<sub>3</sub> compounds<sup>13</sup>.

The hallmarks of strong correlations such as the band narrowing and lower Hubbard bands observed in SrVO<sub>3</sub> which might be expected to be even more easily resolvable in the photoemission on ruthenates due to the larger mass enhancement, thus turn experimentally more elusive to find. On the other hand, the ruthenates have been also pictured as influenced substantially by the proximity

TABLE I: Effects of electron correlation in transition-metal oxides. The values of  $\gamma$ ,  $\gamma/\gamma_b$  ( $= m^*/m_b$ ), and  $W_b/W^*$  are given. The values without reference numbers are from this work.

	$\gamma$ (mJ/K <sup>2</sup> mol)	$\gamma/\gamma_b$ ( $= m^*/m_b$ )	$W_b/W^*$
SrVO <sub>3</sub> ( $t_{2g}^1$ )	8.182 <sup>a</sup>	$\sim 2$ <sup>a</sup>	$\sim 2$ <sup>b</sup>
SrRuO <sub>3</sub> ( $t_{2g}^4$ )	36.3 <sup>c</sup>	$\sim 4$ <sup>c</sup>	$\sim 1$ <sup>d</sup>
Sr <sub>2</sub> RuO <sub>4</sub> ( $t_{2g}^4$ )	39 <sup>e</sup>	$\sim 4$ <sup>f</sup>	$\sim 1$ <sup>g</sup>
SrMoO <sub>3</sub> ( $t_{2g}^2$ )	7.9 <sup>h</sup>	$\sim 2$	$\sim 1$

<sup>a</sup>Ref. 5    <sup>b</sup>Ref. 4    <sup>c</sup>Ref. 9    <sup>d</sup>Ref. 7  
<sup>e</sup>Ref. 10    <sup>f</sup>Ref. 11    <sup>g</sup>Ref. 12    <sup>h</sup>Ref. 18

to the magnetic transition and the corresponding magnetic fluctuations<sup>16</sup> which brings to the problem ingredients whose photoemission signatures are understood less well.

In this context, it is important and interesting to study the effects of electron correlation in another perovskite-type 4d oxide SrMoO<sub>3</sub>, which is a Pauli paramagnetic metal<sup>17</sup> and is therefore expected to show electron correlation free from possible effects of magnetism and superconductivity. Molybdates are particle-hole analogues of ruthenates as far as the occupancy of the  $t_{2g}$  shell is concerned: in SrMoO<sub>3</sub> ( $4d^2$ ) the  $t_{2g}$  band is occupied by two electrons, and in SrRuO<sub>3</sub> (low-spin  $4d^4$ ) the  $t_{2g}$  band is occupied by two holes.

In this paper, we investigate the correlated density-of-states (DOS) of SrMoO<sub>3</sub> experimentally with photoemission and compare the results to the band-structure calculations within local-density approximation (LDA) and the LDA combined with the dynamical mean-field theory (LDA+DMFT). We also compare the results to the analogous ones on SrVO<sub>3</sub>. The comparison between SrMoO<sub>3</sub> and SrVO<sub>3</sub> can be expected to be particularly revealing. First, both materials are paramagnets. Second, both have intermediate degrees of correlations, judging from the effective mass ( $m^*/m_b$ ). Finally these two materials have overall similar band-structure at the level of local density approximation (LDA) as shown in Fig. 3, and a low filling of the  $d$ -shell:  $d^2$  and  $d^1$ , respectively, which means that unlike ruthenates they are not affected that much by the possible effects of proximity to the van-Hove singularity, see, e.g. Ref.<sup>29</sup>.

Nagai *et al.*<sup>18</sup> reported that SrMoO<sub>3</sub> single crystals grown in ultra-low oxygen pressure show resistivity as low as 5.1  $\mu\Omega\text{cm}$  at 300 K. Recently, Radetinac *et al.*<sup>19</sup> reported the fabrication of high-quality SrMoO<sub>3</sub> thin films using argon gas in the pulsed laser deposition (PLD) process. In this study, we fabricated the same type of thin film which has atomic-level flatness at the surface (with a root-mean-square roughness of 0.2 nm<sup>19</sup>) and performed hard x-ray (HX) photoemission spectroscopy measurements. By applying bulk-sensitive HX photoemission spectroscopy to the atomically flat surface, we succeeded

in obtaining the spectrum of bulk Mo 4d bands. The obtained bulk Mo 4d bands do not show band narrowing from the band-structure calculations. This behavior, which is also observed for SrRuO<sub>3</sub>, can be understood if the genuine coherent quasiparticle peak exists only near the Fermi level. This result is an experimental manifestation of the recent DMFT with Hund's rule coupling in Ref.<sup>14,15</sup>, demonstrating that in the case of  $t_{2g}^2$  or  $t_{2g}^4$  systems the overall  $d$  bandwidth is not strongly affected by electron correlations. In the theoretical part of the paper we report further DMFT model calculations that show explicitly that the Hubbard bands are pulled to lower energies by the Hund's rule coupling and that the spectral weight is redistributed within the quasiparticle band instead of being shifted to the Hubbard satellites as is the case in SrVO<sub>3</sub>. Similar results have been discussed also for iron-based superconductors<sup>20</sup>.

We also performed realistic LDA+DMFT calculations of SrMoO<sub>3</sub>. The calculated  $t_{2g}$  spectral functions do not show obvious band narrowing on large ( $\sim 1$  eV) energy scales, yet the low-energy spectra is renormalized, in agreement with measurements. Comparison of the theory to the measurements reveals additional spectral weight at  $\sim -2$  eV that is not present in the theory. We argue that this is not the lower Hubbard band but rather a plasmon satellite, an interpretation that is supported by the existence of satellites in the measured core-level spectra.

The paper is structured as follows. In Sec. II we describe the experimental procedure and in Sec. III we describe some details of the theoretical work. In Sec. IV we report the photoemission results and compare them to what is found in the band-structure LDA and LDA+DMFT calculations. Section V contains discussion of our results and in Sec. VI we conclude. In Appendix A we give LDA+DMFT self-energies and discuss LDA+DMFT results in more details. Appendix B contains DMFT results for a model system that shows explicitly how Hubbard bands are pulled in by the Hund's rule coupling, which supports our interpretation of the experimental spectra.

## II. EXPERIMENT

The SrMoO<sub>3</sub> thin film was grown in the (001) direction on a GdScO<sub>3</sub> (110) substrate [ $(a = 5.482$  Å,  $b = 5.742$  Å, and  $c = 7.926$  Å for the orthorhombic lattice ( $\bar{a} = 3.967$  Å for a pseudocubic lattice definition)] by the PLD method. Since the lattice constant of the cubic SrMoO<sub>3</sub> is 3.976 Å<sup>25</sup>, a lattice mismatch between substrate and film is only  $-0.2$  %. The thickness of the thin film was about 70 nm. The details of the fabrication were described in Ref.<sup>19</sup>.

HX photoemission measurements were carried out at BL-47XU of SPring-8. No surface cleaning was performed before the measurements. The HX photoemission spectra were recorded using a Scienta R-4000 electron en-

ergy analyzer with a total energy resolution of 300 meV at the photon energy of 7.94 keV. We also performed SX photoemission measurements at Photon Factory BL-2C to obtain the information about surface states. The SX photoemission spectra were recorded using a Scienta SES-2002 electron energy analyzer with a total energy resolution of 300 meV at the photon energy of 780 eV. The position of  $E_F$  was determined by measuring the spectra of gold which was in electrical contact with the sample. All the spectra were measured at room temperature.

### III. THEORY

The band structure was calculated using the linearized augmented plane wave method implemented in the WIEN2K package. Bulk SrMoO<sub>3</sub> has an orthorhombic crystal structure below 150 K, a tetragonal one between 150 K and 250 K, and cubic structure at temperatures above 250 K<sup>25</sup>. The degree of distortions away from cubic symmetry in this compound is small, and we found that the band structure of the compound is not influenced by distortions significantly. The results which we report below are for the cubic perovskite structure with the lattice constant  $a = 3.976 \text{ \AA}$ <sup>25</sup>. The LDA+DMFT calculations were done in the framework described in Ref.<sup>21,22</sup>. Full rotationally invariant interaction with Kanamori parameters  $U = 3.0 \text{ eV}$  and  $J = 0.3 \text{ eV}$  has been used<sup>23</sup>. Using these parameters, the calculated mass enhancement is  $\sim 2$ , consistent with experiment. The analytical continuations of the data to real frequencies were performed using stochastic maximum entropy method<sup>24</sup>.

To support our interpretation of the results, we also carried out the model calculations within DMFT, which were done using the semicircular DOS.

### IV. PHOTOEMISSION RESULTS; COMPARISON TO LDA AND LDA+DMFT

Figure 1 shows the core-level photoemission spectra of the SrMoO<sub>3</sub> thin film. The O 1s spectrum (a) shows that the ‘‘contamination’’ signal on the higher binding-energy side is weak. The Sr 3d spectrum (b) has only one component at  $3d_{5/2}$  and  $3d_{3/2}$ . These two results demonstrate that our photoemission spectra are free from surface degradation or contamination and represent the bulk electronic properties of the SrMoO<sub>3</sub> thin film. The Mo 3d spectrum (c) has two structures at  $-229.3 \text{ eV}$  and  $-232.5 \text{ eV}$ , almost the same as those of MoO<sub>2</sub> (Mo<sup>4+</sup>)<sup>26</sup>, representing the bulk Mo<sup>4+</sup> states. This core level was also measured at 780 eV in the SX region, and two structures were observed at  $-233.3 \text{ eV}$  and  $-236.4 \text{ eV}$ , almost the same as those of MoO<sub>3</sub> (Mo<sup>6+</sup>)<sup>26</sup>. It also has some weak Mo<sup>4+</sup> signal at  $-229.3 \text{ eV}$ . These results mean that our thin film had Mo<sup>4+</sup> in bulk and the surface states were dominated by Mo<sup>6+</sup>. Since Mo<sup>6+</sup> has no 4d elec-

trons, such surface oxidized states do not affect the Mo 4d band which will appear in subsequent figures.

There is also some additional intensity in all the core levels, that is, at  $-532.5 \text{ eV}$  in O 1s (a), at  $-138 \text{ eV}$  in Sr 3d (b), and at  $-235 \text{ eV}$  in Mo 3d (c). We plotted these three core levels as a function of relative energy to the main peak in Fig. 1 (d). One can see the intensity around  $-2 \text{ eV}$  in all the core levels, which points to a common origin. As we discuss in more detail later, we believe that these structures are due to plasmon satellite. The energy of  $\sim 2 \text{ eV}$  coincides closely with the plasma frequency reported in the measurements of reflectivity<sup>27</sup>.

Figure 2 (a) shows the valence-band photoemission spectrum of the SrMoO<sub>3</sub> thin film. By comparing the photoemission spectrum with the DOS deduced from the LDA (b), one can see that the Mo 4d band is located near  $E_F$ , and the O 2p band is located on the higher-energy side (from  $-4$  to  $-10 \text{ eV}$ ). The dashed line in panel (a) shows the tail of the O 2p band extended towards the Mo 4d band. One can also clearly see the Mo 4d band crossing  $E_F$  and that the photoemission signal is described well by the LDA DOS.

Figure 3 (a) shows the bulk  $d$  orbital component obtained by subtracting the oxygen contribution (dashed line in Fig. 2 (a)) from the photoemission signal. This photoemission DOS is compared to the results from the LDA band-structure calculation for SrMoO<sub>3</sub> as well as to the  $t_{2g}$  DOS from the LDA+DMFT calculation, which includes the effects of correlation. The results for SrVO<sub>3</sub> are also shown in panel (b), where the experimental spectrum is taken from Ref.<sup>4</sup>. The calculated DOS has been broadened with a Gaussian of 0.3 eV (FWHM: a full width at half maximum) and an energy-dependent Lorentzian (FWHM =  $0.2|E - E_F| \text{ eV}$ )<sup>30</sup> to account for the instrumental resolution and the lifetime broadening of the photohole, respectively. The theoretical data was multiplied by the Fermi function.

The first observation is that the experimental photoemission is distinct from the LDA results, which is a signature of electronic correlations. In the case of SrVO<sub>3</sub>, these manifest in an obvious, well-known way: the quasiparticle band is narrowed and a split-off lower Hubbard band is seen. These results are reproduced very well by the LDA+DMFT.

In the case of SrMoO<sub>3</sub>, the electronic correlations manifest in a different way. The observed photoemission does not show band narrowing. Rather, the quasiparticle band appears to be widened and develops a hump at energy  $-2.5 \text{ eV}$ .

The LDA+DMFT data also does not display an obvious band narrowing and is consistent with experiment above  $-1 \text{ eV}$ . Whereas part of the spectral weight extends also to frequencies below  $-2 \text{ eV}$  due to the large imaginary part of the self energy found in this energy range (for the self energies as well as about the spectra at positive frequencies, see Appendix A), our LDA+DMFT calculations cannot account for the experimental excess weight at  $\sim -2.5 \text{ eV}$ . This leads us to propose that the hump

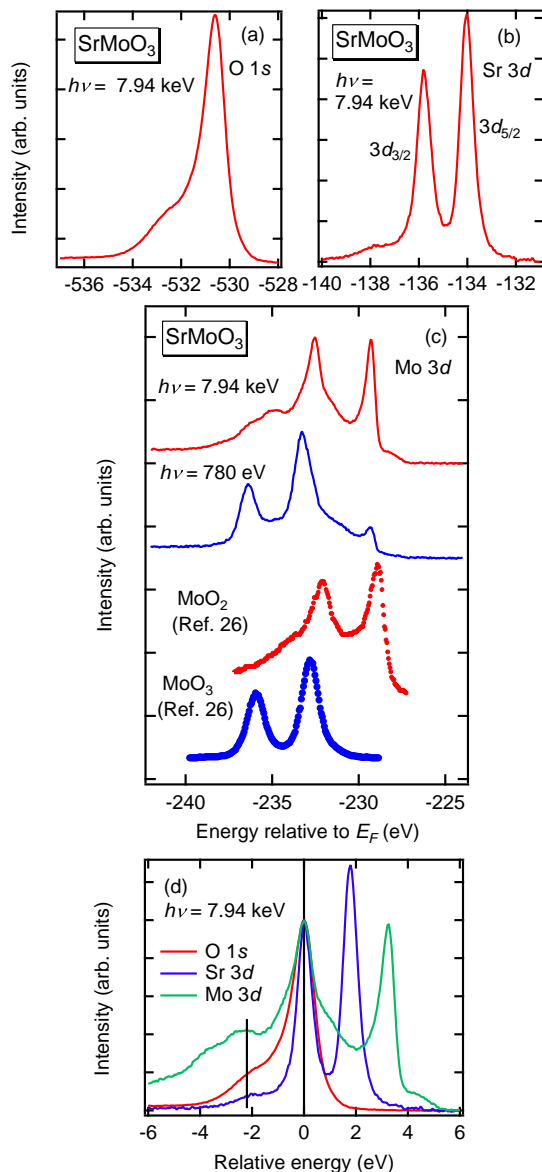


FIG. 1: (Color online): Core-level photoemission spectra of the SrMoO<sub>3</sub> thin film. (a) O 1s. (b) Sr 3d. (c) Mo 3d. Mo 3d spectra were measured by both HX and SX, plotted together with the reference spectra of MoO<sub>2</sub> and MoO<sub>3</sub> (Ref. 26). Panel (d) shows all the core levels plotted as a function of relative energy to the main peak.

is not a Hubbard band. Note also that the hump occurs at an energy which is separated more from the Fermi energy than the Hubbard band in SrVO<sub>3</sub>, whereas the interaction parameters are expected to be smaller for 4d elements than for 3d elements due to the more extended orbitals of the former. Weaker electronic correlation in 4d TMOs CaRuO<sub>3</sub> and SrRuO<sub>3</sub> than 3d TMOs were reported in Ref. 31 from the comparison between photoemission spectra and first-principles calculations.

What is then the origin of the hump? Whereas more

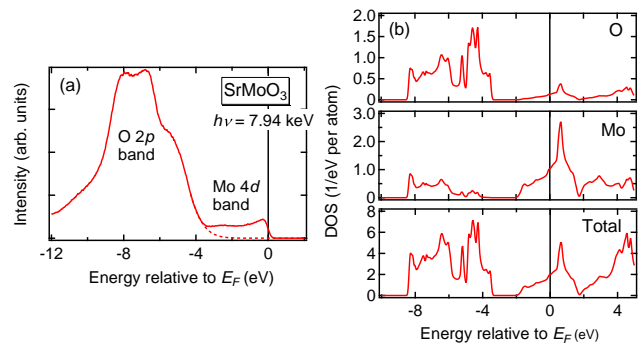


FIG. 2: (Color online): Electronic structure of SrMoO<sub>3</sub> near the Fermi level. (a) Valence-band photoemission spectrum of a SrMoO<sub>3</sub> thin film. The dashed line shows the estimated tail of the O 2p band. (b) The DOS of SrMoO<sub>3</sub> obtained from band-structure calculations.

work will be needed to clarify this conclusively, we believe the most natural explanation is that it is a plasmon satellite. The plasma edge in the optical experiments<sup>27</sup> is indeed at about 2 eV, and we stress again that the satellite structures are seen also in all the core levels. Influence of plasmons in core-level photoemission spectra was observed in simple metals like Mg<sup>32,33</sup> and conducting oxides like Na<sub>x</sub>WO<sub>3</sub><sup>34</sup> and K<sub>0.3</sub>MoO<sub>3</sub><sup>35</sup>. In correlated materials the influence of plasmons on photoemission is discussed less often. We note that the plasma frequencies are about 2 eV, which means that they often overlap with the Hubbard band and that therefore 4d oxides that do not show pronounced Hubbard bands might be promising materials to investigate plasmons further. Molybdates, that have a gap in the LDA spectrum between -3 and -2 eV are particularly promising in this respect.

## V. DISCUSSION

We now turn to the origin of the difference observed in photoemission between SrMoO<sub>3</sub> and SrVO<sub>3</sub>. Why does the latter exhibit a narrowed quasiparticle band and the Hubbard satellites and the latter not?

Recently, de' Medici *et al.*<sup>14,15</sup> calculated the quasiparticle weight  $Z$  in  $t_{2g}$  systems by including the effects of Hund's rule coupling  $J$ . The results for  $t_{2g}^1$  and  $t_{2g}^2$  are reproduced in Fig. 4, where  $U$  is the on-site Coulomb interaction and  $D$  is the half bandwidth. There is a marked difference between the  $t_{2g}^1$  and  $t_{2g}^2$  systems. In the case of the  $t_{2g}^1$  system, a non-zero  $J$  increases  $Z$ , whereas in the case of the  $t_{2g}^2$ ,  $t_{2g}^4$  systems a non-zero  $J$  rather decreases  $Z$  (unless  $U/W$  is too large). This means that in the latter case even small values of  $U/W \lesssim 1$  may lead to a suppressed  $Z$  at small energy scales. Because so small values of  $U$  are sufficient to suppress  $Z$ , the high energy scales cannot be separated from the small energy scales in a clear way and instead of the narrowing of the

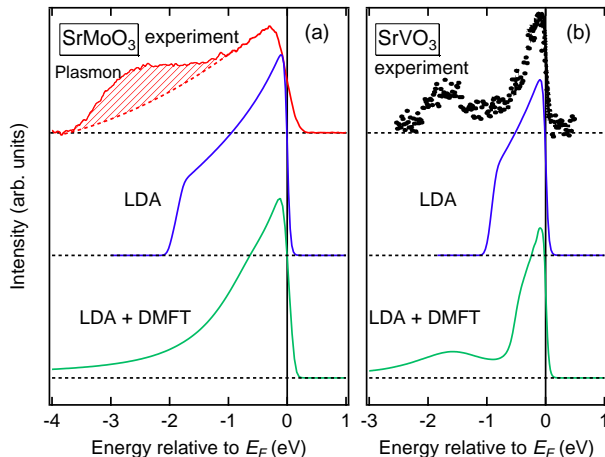


FIG. 3: (Color online): Comparison of the bulk component obtained by photoemission spectroscopy and the band-structure calculation for SrMoO<sub>3</sub> (a) and SrVO<sub>3</sub> (b). The experimental spectrum of SrVO<sub>3</sub> is from Ref.<sup>4</sup>. The calculated DOS has been broadened with a Gaussian and a Lorentzian function. The hump structure at  $-2.5$  eV in experiment (a) is attributed to a plasmon satellite.

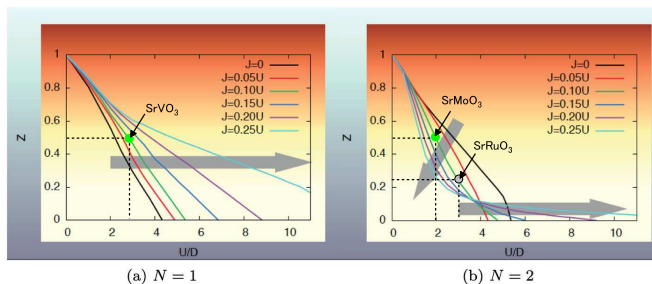


FIG. 4: (Color online): Quasiparticle weight  $Z$  as a function of  $U/D$  for  $N = 1, 2$  electrons in three orbitals<sup>14</sup>. The gray arrows indicate the influence of an increasing Hund's rule coupling  $J/U$ . SrRuO<sub>3</sub>, plotted in  $N = 2$ , is actually a  $d^4$  occupancy and one should note that there is not an electron-hole symmetry for a  $t_{2g}$  DOS.

quasiparticle band, the spectral weight is redistributed within it. This is illustrated in more details by DMFT calculations on a model system in Appendix B.

In the case of SrMoO<sub>3</sub>, we obtain  $\gamma_b = 4.6$  mJ/mol K<sup>2</sup> from the band-structure calculation, and  $\gamma = 7.9$  mJ/mol K<sup>2</sup> from specific heat measurements<sup>18</sup>. These values give  $m^*/m_b = \gamma/\gamma_b \sim 2$ , but this effect of electron correlation is not clearly observed in the photoemission spectra shown in Fig. 3 (a), indicating that the genuine coherent part with band narrowing exists only near  $E_F$  as also suggested for SrRuO<sub>3</sub><sup>7</sup>. In the case of  $t_{2g}^2$  (or  $t_{2g}^4$ ) systems, nonzero  $J$  can decrease  $Z$ , which is opposite to the case of  $t_{2g}^1$ . Small values of  $Z$  is not necessarily realized

by a large value of  $U/D$ . Therefore, the overall  $d$  bandwidth, determined by the value of  $U/D$ , can be rather free from electron correlation effects.

Since  $Z = (\gamma/\gamma_b)^{-1}$ , if we assume  $J = 0.10U$ , we obtain  $U/D \sim 3$  for SrVO<sub>3</sub>, and  $U/D \sim 2$  for SrMoO<sub>3</sub>. One can clearly see that SrVO<sub>3</sub> has a larger value of  $U/D$  and is closer to the Mott transition than SrMoO<sub>3</sub>. This makes the case for SrMoO<sub>3</sub> being a ‘‘Hund’s metal’’ with intermediate correlations and explains the difference in spectra between the two materials shown in Fig. 3.

## VI. CONCLUSION

We have studied the electronic structures of a SrMoO<sub>3</sub> thin film by HX photoemission spectroscopy. From the Mo  $3d$  core level, we found that the valence of Mo is indeed  $4+$  in the bulk. The valence-band spectrum clearly showed the Mo  $4d$  band crossing  $E_F$ . We compared thus obtained bulk Mo  $4d$  band with the band-structure calculation. Although the electronic specific heat shows a clear signature of mass enhancement, we did not observe a band narrowing effect arising from electron correlation effects, suggesting that the genuine coherent part exists only near  $E_F$ . Such a behavior was also observed in SrRuO<sub>3</sub>, and is considered to be an experimental manifestation of the recent DMFT studies including Hund’s rule coupling<sup>14,15</sup>. The LDA+DMFT cannot account for the broad hump at  $\sim -2.5$  eV. The relatively high-binding energy of the feature as well as discrepancy with the LDA+DMFT suggests the hump is not a lower Hubbard band. We believe the hump is a plasmon satellite and propose that molybdates might be an interesting material to investigate physics of plasmons in correlated materials further.

## Acknowledgments

This research was granted by the Japan Society for the Promotion of Science (JSPS) through the ‘‘Funding Program for World-Leading Innovative R&D on Science and Technology (FIRST Program),’’ initiated by the Council for Science and Technology Policy (CSTP). This work was supported in part by JSPS Grant-in-Aid for Scientific Research(S) No. 24224009. The synchrotron radiation experiments at SPring-8 were performed under the approval of the Japan Synchrotron Radiation Research Institute (2010B1740 and 2011A1624). The synchrotron radiation experiments at KEK-PF were performed under the approval of the Program Advisory Committee (Proposal No. 2008S2-003) at the Institute of Materials Structure Science, KEK. The computing time was provided by IDRIS-GENCI under grant 2011091393. JM acknowledges support of the Slovenian Research Agency (ARRS) under Program P1-0044.

## Appendix A: LDA+DMFT DOS and self energies

For SrVO<sub>3</sub> the values of interaction  $U = 4.5$  eV and  $J/U = 0.15$  was used in the calculation. Note that these are the screened values, compatible with the  $t_{2g}$  only calculation that we do here. Starting from the same ratio of atomic interaction parameters,  $J_{\text{atom}}/U_{\text{atom}}$  the screened values of  $J/U$  can be expected to be higher in  $3d$  oxides, because the screening which is stronger in  $3d$  oxides due to the proximity of the oxygen states affects more  $U$  than the  $J$  which is related to higher orders of multipole expansion of the Coulomb interaction.

On top panels of Fig. 5 the LDA+DMFT DOS are compared to the LDA DOS for SrMoO<sub>3</sub> (data shown left) and SrVO<sub>3</sub> (right). In the case of SrVO<sub>3</sub>,  $U/W \sim 2 > 1$ , hence the split-off Hubbard bands are found. In the case of SrMoO<sub>3</sub>,  $U/W \lesssim 1$ , hence the high energy features are merged with the quasiparticle band. More pronounced difference as well as a precursor of the Hubbard band at about 1.5 eV are actually found on the positive frequency side which is invisible to photoemission experiments.

On medium panels of Fig. 5 the real and on bottom panels the imaginary parts of the self energy  $\Sigma$  are shown. For SrMoO<sub>3</sub>, on the negative side, the self energy deviates from the linear behavior at about  $-0.5$  eV and levels off to the frequency independent behavior, recovering the bare LDA dispersion, although with significant broadening ( $\text{Im}\Sigma$ , shown in lower panel) below that frequency. Conversely, for SrVO<sub>3</sub> the imaginary part of the self energy shows a weak pole-like structure, signifying the Hubbard band, and related feature with positive slope in the real part of the self energy in the same energy range.

The magnitude of  $\text{Im}\Sigma$  is found to be comparable at small frequencies (note the data is described well by a parabola with similar curvature). At higher frequencies  $\sim 1$ eV, on the other hand, the magnitude of  $\text{Im}\Sigma$  in SrMoO<sub>3</sub> becomes relatively smaller, which is another manifestation of the fact that the electronic correlations originate from the multiplet splittings which become unimportant at frequencies above  $J$ .

## Appendix B: Model DMFT results

To further support the interpretation of the absence of Hubbard bands in terms of the effects of the Hund's rule coupling, we calculated the correlated DOS for a model with semicircular DOS for several ratios of  $J/U = 0.0, 0.05, 0.1, 0.15$  (with  $J/U = 0.15$  being close to the physical values for the transition-metal oxides), adjusting  $U$  so that the low frequency mass renormalization remains constant  $m^*/m = Z^{-1} \approx 4$ .

The calculated DOS are shown on Fig. 6. At  $J/U = 0$ , for sizable correlations to occur, the interaction strength must be tuned quite close to the Mott transition (which occurs for  $U/D \approx 5.5$ ). The resulting spectra are akin to the spectra of doped Mott insulators: pronounced Hubbard bands and the narrow quasiparticle peak, implying

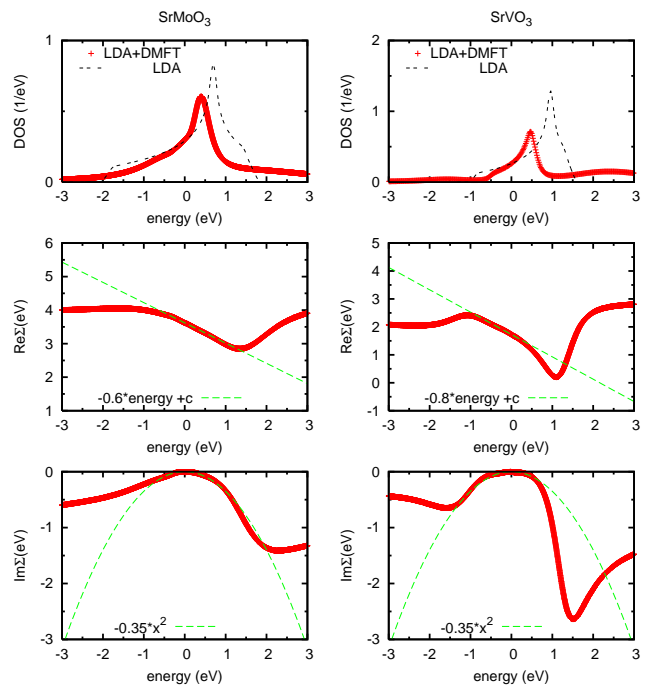


FIG. 5: Top panels: LDA and LDA+DMFT DOS for SrMoO<sub>3</sub> (left) and SrVO<sub>3</sub> (right). Medium panels: Real parts of self energy. Linear fit is also shown. Bottom panels: Imaginary parts of the self energy. Parabolic fit is also shown.

clear separation of high and low energy scales.

As  $J/U$  is increased, two effects occur. First, as the correlations due to  $J$  develop a smaller value of  $U$  is sufficient to reach the same degree of renormalization. Second, the effective atomic interaction for a transfer of electron, given by  $E(N+1) + E(N-1) - 2E(N)$  that is equal to  $U - 3J$  for a  $t_{2g}$  atom away from half-filling, is diminished even more with increasing  $J/U$ , thus the Hubbard bands are pulled in by the Hund's rule coupling  $J$ .

This is reflected in the spectra by the diminishing of the peak-to-peak distance between the Hubbard bands (4.7, 3.7, 2.7, 2.1 in units of  $D$  for increasing  $J/U = 0.0, \dots, 0.15$ , respectively). At the largest  $J/U = 0.15$  considered, the lower Hubbard band starts to overlap with the quasiparticle band and remains visible only as a mild shoulder. The upper Hubbard band, however, remains visible. The high-energy and the low-energy scales are not separated clearly anymore, the incoherent spectral weight is transferred to energies which overlap with the quasiparticle band and therefore influence its shape. The quasiparticle peak appears broader and obtains an asymmetric shape. In the inset, we replot the DOS in the narrower frequency range. The quasiparticle peak at  $J/U = 0.15$  has markedly different shape from that of the  $J/U = 0$  case, whose shape closely resembles that of the narrowed noninteracting (semicircular) DOS. Next to the stochastic maximum entropy analytical continuation we show also the data obtained by the Padé approxi-

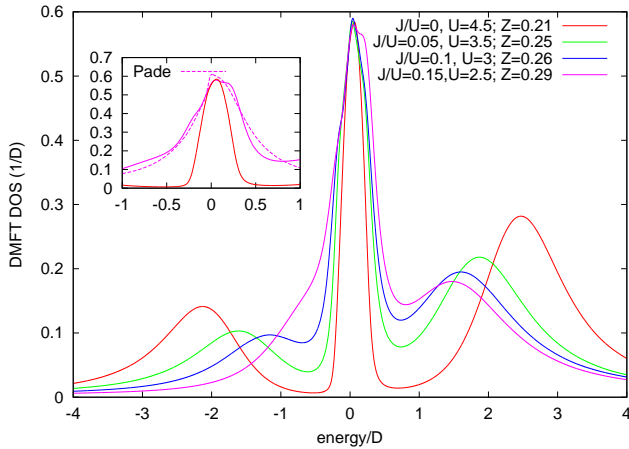


FIG. 6: The DMFT DOS for the  $t_{2g}$  model with semicircular noninteracting DOS occupied by 2 electrons/atom. Several values of  $J/U$  were used and  $U$  is adjusted so that the quasiparticle renormalization is close to  $Z = 1/4$ . Inset: close-up on quasiparticle peak for  $J/U = 0, 0.15$ . For  $J/U = 0.15$ , also the Padé data is shown for comparison. Other curves are obtained using maximum entropy analytical continuation.

mants. The broadened quasiparticle peak with asymmetric shape is seen from both analytical continuations, which therefore is likely a genuine feature of Hund's metals and which deserves further exploration.

On Fig. 7 we show the self energies for  $J/U = 0$  and  $J/U = 0.15$ . The real part of the self energies exhibit similar low frequency slope, which corresponds to the matching quasiparticle residue  $Z$ , but in other aspects the data for  $J/U = 0.15$  differs substantially from the data at vanishing Hund's coupling strength. The  $J/U = 0$  real part of the self energy follows a quasi-linear dependence up to a high energy scale followed by an abrupt feature indicating the onset of the Hubbard band. Conversely, for  $J/U = 0.15$  the real part of the self energy is linear only up to a small frequency scale. At higher frequencies relatively mild frequency dependence is seen, which indicates a weaker overall band narrowing. Except on approaching the Hubbard bands, the magnitude of  $\text{Im}\Sigma$  (bottom inset) for  $J/U = 0.15$  is larger, indicating correlations that develop due to the Hund's rule coupling despite a significantly smaller value of  $U$ . The genuine

coherent, but strongly renormalized part, is thus actually limited to the low frequency scales ( $\lesssim 0.1D$  for the present data), whereas at higher frequency scales a larger dispersion, but with much shorter lifetime is recovered.

Interesting further insight into the particular behavior of self energies for Hund's metals is obtained by considering Kramers-Kronig relations. Take that  $\text{Im}\Sigma = -A\omega^2$  up to a cutoff  $\omega_c$ , and that it vanishes at  $|\omega| > \omega_c$ . Kramers-Kronig relations give  $\text{Re}\Sigma = -2\omega_c A\omega + \dots$ . The slope of  $\text{Re}\Sigma$  which determines the quasiparticle renormalization increases both with  $\omega_c$  and  $A$ . At a fixed quasiparticle renormalization, this relation also tells that

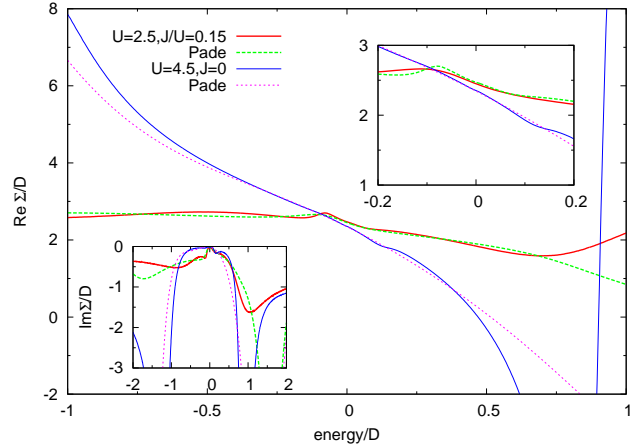


FIG. 7: The DMFT self energies for the  $t_{2g}$  model for  $J/U = 0$  and  $J/U = 0.15$ . Analytical continuations using Padé approximants and maximum entropy method are shown. The  $J/U = 0$  results are shifted vertically for easier comparison between the two datasets. Top inset: close-up to low frequencies. Bottom inset: imaginary part of self energies.

the cutoff frequency (which has the meaning of the energy of the kink) and the curvature are related. For vanishing Hund's rule coupling, the curvature of  $\text{Im}\Sigma$  is small but persists up to a larger cutoff. For physical values of  $J$ , the curvature is larger, but it holds only up to a small frequency scale. This explains why in Hund's metals, like ruthenates, the kinks are often found (see, e.g.<sup>29</sup> and references therein) at small energy scales.

\* Electronic address: wadati@ap.t.u-tokyo.ac.jp;

URL: <http://www.geocities.jp/qxbqd097/index2.htm>

<sup>1</sup> M. Imada, A. Fujimori, and Y. Tokura, Rev. Mod. Phys. **70**, 1039 (1998).

<sup>2</sup> A. Fujimori, I. Hase, H. Namatame, Y. Fujishima, Y. Tokura, H. Eisaki, S. Uchida, K. Takegahara, and F. M. F. de Groot, Phys. Rev. Lett. **69**, 1796 (1992).

<sup>3</sup> I. H. Inoue, I. Hase, Y. Aiura, A. Fujimori, Y. Haruyama, T. Maruyama, and Y. Nishihara, Phys. Rev. Lett. **74**, 2539

(1995).

<sup>4</sup> A. Sekiyama, H. Fujiwara, S. Imada, S. Suga, H. Eisaki, S. I. Uchida, K. Takegahara, H. Harima, Y. Saitoh, I. A. Nekrasov, G. Keller, D. E. Kondakov, A. V. Kozhevnikov, T. Pruschke, K. Held, D. Vollhardt, and V. I. Anisimov, Phys. Rev. Lett. **93**, 156402 (2004).

<sup>5</sup> I. H. Inoue, O. Goto, H. Makino, N. E. Hussey, and M. Ishikawa, Phys. Rev. B **58**, 4372 (1998).

<sup>6</sup> A. Callaghan, C. W. Moeller, and R. Ward, Inorg. Chem.

- 5, 1572 (1966).
- <sup>7</sup> M. Takizawa, D. Toyota, H. Wadati, A. Chikamatsu, H. Kumigashira, A. Fujimori, M. Oshima, Z. Fang, M. Lippmaa, M. Kawasaki, and H. Koinuma, *Phys. Rev. B* **72**, 060404(R) (2005).
  - <sup>8</sup> P. B. Allen, H. Berger, O. Chauvet, L. Forro, T. Jarlborg, A. Junod, B. Revaz, and G. Santi, *Phys. Rev. B* **53**, 4393 (1996).
  - <sup>9</sup> J. Okamoto, T. Mizokawa, A. Fujimori, I. Hase, M. No-hara, H. Takagi, Y. Takeda, and M. Takano, *Phys. Rev. B* **60**, 2281 (1999).
  - <sup>10</sup> Y. Maeno, H. Hashimoto, K. Yoshida, S. Nishizaki, T. Fujita, J. G. Bednorz, and F. Lichtenberg, *Nature* **372**, 532 (1994).
  - <sup>11</sup> T. Oguchi, *Phys. Rev. B* **51**, 1385 (1995).
  - <sup>12</sup> Z. V. Pchelkina, I. A. Nekrasov, T. Pruschke, A. Sekiyama, S. Suga, V. I. Anisimov, and D. Vollhardt, *Phys. Rev. B* **75**, 035122 (2007).
  - <sup>13</sup> K. Maiti and R. S. Singh, *Phys. Rev. B* **71**, 161102 (2005).
  - <sup>14</sup> L. de' Medici, J. Mravlje, and A. Georges, *Phys. Rev. Lett.* **107**, 256401 (2011).
  - <sup>15</sup> A. Georges, L. de' Medici, and J. Mravlje, *Annu. Rev. Cond. Mat. Phys.* **4**, 137 (2013).
  - <sup>16</sup> G. Cao, W. Song, Y. Sun and X. Lin, *Solid State Communications* **131**, 331 (2004).
  - <sup>17</sup> G. H. Bouchard and M. J. Sienko: *Inorg. Chem.* **7**, 441 (1968).
  - <sup>18</sup> I. Nagai, N. Shirakawa, S. Ikeda, R. Iwasaki, H. Nishimura, and M. Kosaka, *Appl. Phys. Lett.* **87**, 024105 (2005).
  - <sup>19</sup> A. Radetinac, K. S. Takahashi, L. Alff, M. Kawasaki, and Y. Tokura, *Appl. Phys. Express* **3**, 073003 (2010).
  - <sup>20</sup> A. Kutepov, K. Haule, S. Y. Savrasov, and G. Kotliar, *Phys. Rev. B* **82**, 045105 (2010).
  - <sup>21</sup> M. Aichhorn, L. Pourovskii, V. Vildosola, M. Ferrero, O. Parcollet, T. Miyake, A. Georges and S. Biermann, *Phys. Rev. B* **80**, 085101 (2009).
  - <sup>22</sup> M. Ferrero and O. Parcollet, TRIQS: <http://ipht.cea.fr/triqs>.
  - <sup>23</sup> L. Vaugier, H. Jiang, and S. Biermann, *Phys. Rev. B* **86**, 165105 (2012).
  - <sup>24</sup> K. S. D. Beach, *cond-mat/0403055*.
  - <sup>25</sup> R. B. Macquart, B. J. Kennedy, and M. Avdeev, *J. Solid State Chem.* **183**, 249 (2010).
  - <sup>26</sup> R. J. Colton, A. M. Guzman, and J. W. Rabalais, *J. Appl. Phys.* **49**, 409 (1978).
  - <sup>27</sup> H. Mizoguchi, N. Kitamura, K. Fukumi, T. Mihara, J. Nishii, M. Nakamura, N. Kikuchi, H. Hosono, and H. Kawazoe, *J. Appl. Phys.* **87**, 4617 (2000).
  - <sup>28</sup> J. P. Perdew, K. Burke, and M. Ernzerhof, *Phys. Rev. Lett.* **77**, 3865 (1996).
  - <sup>29</sup> J. Mravlje, M. Aichhorn, T. Miyake, K. Haule, G. Kotliar, and A. Georges, *Phys. Rev. Lett.* **106**, 096401 (2011).
  - <sup>30</sup> H. Hochst, P. Steiner, G. Reiter, and S. Hufner, *Z. Phys. B* **42**, 199 (1981).
  - <sup>31</sup> K. Maiti and R. S. Singh, *Phys. Rev. B* **71**, 161102(R) (2005).
  - <sup>32</sup> L. Ley, F. R. McFeely, S. P. Kowalczyk, J. G. Jenkin, and D. A. Shirley, *Phys. Rev. B* **11**, 600 (1975).
  - <sup>33</sup> L. Ley and M. Cardona, *Photoemission in Solids II* (Springer-Verlag, Berlin, 1979).
  - <sup>34</sup> J.-N. Chazalviel, M. Campagna, G. K. Wertheim, and H. R. Shanks, *Phys. Rev. B* **16**, 697 (1977).
  - <sup>35</sup> G. K. Wertheim, L. F. Schneemeyer, and D. N. E. Buchanan, *Phys. Rev. B* **32**, 3568 (1985).